Robert Panish
18.086
May 12, 2008

Exploration of shock formation for a reentering space shuttle
Final Report

1 Introduction

During reentry into the Earth's atmosphere, NASA's space shuttle must decelerate from an orbital velocity of 17,500MPH to a subsonic flight regime where it can land on a conventional runway. When it first enters the atmosphere at an altitude of over 250,000 feet, the shuttle is traveling at Mach 25, or 25 times the speed of sound.

Any object entering an atmosphere is subject to intense heating caused by the aerodynamic friction with the steadily thickening air. Traveling at hypersonic speeds, a pointed spacecraft will have shock waves form from the nose of the vehicle, as shown in the upper left plot of the figure below.

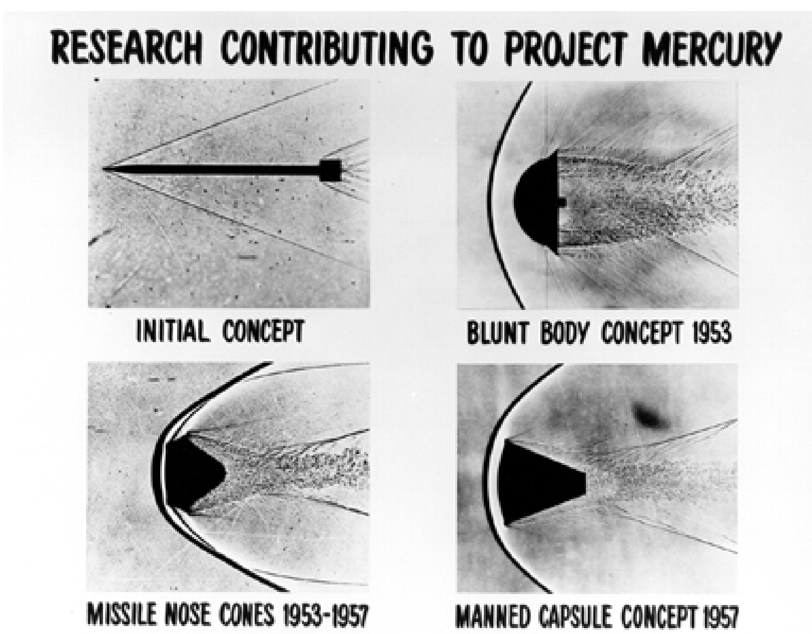

An innovative idea by Dr. Julian Allen in 1953 proposed that a blunt body would be able to withstand a more intense reentry profile. The reason for this is that the shock wave becomes detached from the nose of the vehicle and forms a *bow shock* as shown in the three other plots above. A bow shock wave serves to decrease the severity of the atmospheric friction by diverting some of the flow away from the vehicle. All spacecraft use blunt-body geometry to survive reentry.

The space shuttle has a complex geometry, but it behaves essentially as a blunt-body reentry vehicle during the most intense part of reentry. The shock waves that form are crucial for protecting the shuttle. The shuttle enters the atmosphere with the blunt underside of the orbiter taking the brunt of the aerodynamic heating. It enters at an angle of attack of approximately 15 degrees. The shuttle is protected from the intense heat of reentry by the Thermal Protection System (TPS). Ceramic tiles absorb the heat and protect the aluminum superstructure. The TPS is composed of high temperature tiles (black in color) and low temperature tiles and blankets (white). The tile thickness varies along the vehicle depending on how much heating is expected. A single protruding object from the bottom of the shuttle could disrupt the designed shock wave configuration, creating a heat concentration that may destroy the vehicle.

2 Problem Description

The goal of this project is to model the shock wave formation on the space shuttle during reentry. A two dimensional model of the space shuttle is used to investigate exactly where the shock waves form during reentry. Only a steady state solution is examined where the shock waves have already formed and the free stream conditions are not changing with time. A number of methods are used in industry to predict the shock locations on a hypersonic vehicle, but I am interested in using the Shock Capturing Technique (SCT). SCT requires no a priori estimate of the shock locations and uses a finite difference method to calculate the shock locations given only the free stream flow conditions and the vehicle geometry.

2.1 Justification of 2D Model

A two dimensional model was chosen for a variety of reasons. Primarily, creating a 3D model of the space shuttle, with calculated derivatives at each point, is exceedingly difficult and beyond the scope of this project. A 2D model should provide reasonable results in certain areas on the shuttle. For a flight profile with small slide slip, the flow along the centerline of the vehicle should be entirely two dimensional. For the purposes of this project, analysis will be performed along the centerline. Along the centerline, a 3D model would provide the same results with no greater understanding of the numerical principles.

3 Compressible Flow Theory

For slow air velocities, it is a reasonable assumption to consider air to be incompressible. However, for velocities greater than about Mach 0.3, three-tenths the speed of sound, air must be considered to be compressible. In a compressible flow problem, the density of the fluid is not constant. Compressible fluid dynamics are very different from incompressible flow and much of the intuition developed for incompressible problems is not applicable. In particular, when a supersonic flow encounters an obstacle such as an aircraft wing, a shock wave occurs which serves to redirect the flow around the obstacle.

Anderson[1] derives the conservation form of the governing equations for steady, three-dimensional flow, which are given by

$$\frac{\partial\left(\rho u\right)}{\partial x}+\frac{\partial\left(\rho v\right)}{\partial y}+\frac{\partial\left(\rho w\right)}{\partial z}=0 \tag{1}$$

$$\frac{\partial}{\partial x}\left(\rho u^2+p\right)+\frac{\partial\left(\rho uv\right)}{\partial y}+\frac{\partial\left(\rho uw\right)}{\partial z}=\rho f_x \tag{2}$$

$$\frac{\partial\left(\rho vu\right)}{\partial x}+\frac{\partial}{\partial y}\left(\rho v^2+p\right)+\frac{\partial\left(\rho vw\right)}{\partial z}=\rho f_y \tag{3}$$

$$\frac{\partial\left(\rho wu\right)}{\partial x}+\frac{\partial\left(\rho wv\right)}{\partial y}+\frac{\partial}{\partial z}\left(\rho w^2+p\right)=\rho f_z \tag{4}$$

$$\frac{\partial}{\partial x}\left[\rho\left(e+\frac{V^2}{2}\right)u+pu\right]+\frac{\partial}{\partial y}\left[\rho\left(e+\frac{V^2}{2}\right)v+pv\right]+\frac{\partial}{\partial z}\left[\rho\left(e+\frac{V^2}{2}\right)w+pw\right]=\rho\dot{q}+\rho\left(uf_x+vf_y+wf_z\right) \tag{5}$$

where u, v, and w are the flow velocities in the x, y, and z directions, respectively, ρ is the fluid density, p is the pressure, e is the potential energy per unit mass, and $V=\sqrt{u^2+v^2+w^2}$.

These equations may be expressed in a more compact form

$$\frac{\partial F}{\partial x}+\frac{\partial G}{\partial y}+\frac{\partial H}{\partial z}+J=0 \tag{6}$$

where

$$F = \begin{bmatrix} \rho u \\ \rho u^2 + p \\ \rho v u \\ \rho w u \\ \rho \left(e + \frac{V^2}{2} \right) u + p u \end{bmatrix} \qquad G = \begin{bmatrix} \rho v \\ \rho v u \\ \rho v^2 + p \\ \rho w v \\ \rho \left(e + \frac{V^2}{2} \right) v + p v \end{bmatrix}$$

$$H = \begin{bmatrix} \rho w \\ \rho u w \\ \rho v w \\ \rho w^2 + p \\ \rho \left(e + \frac{V^2}{2} \right) w + p w \end{bmatrix} \qquad J = \begin{bmatrix} 0 \\ \rho f_x \\ \rho f_y \\ \rho f_z \\ \rho \dot{q} + \rho \left(u f_x + v f_y + w f_z \right) \end{bmatrix}$$

The J term is the source term, which is taken to be zero for this exercise. And for two dimensional flow with no source term Equation 6 reduces to

$$\frac{\partial F}{\partial x} = -\frac{\partial G}{\partial y} \tag{7}$$

where

$$F = \begin{bmatrix} \rho u \\ \rho u^2 + p \\ \rho v u \\ \rho \left(e + \frac{V^2}{2} \right) u + p u \end{bmatrix} \qquad G = \begin{bmatrix} \rho v \\ \rho v u \\ \rho v^2 + p \\ \rho \left(e + \frac{V^2}{2} \right) v + p v \end{bmatrix}$$

These equations are in conservation form [2], that is the entries in F and G are flux variables. The primitive variables u, v, p, ρ, and e may be solved from F or G with the addition of one more relation derived from the ideal gas law.

$$p = \rho e \left(\gamma - 1 \right) \tag{8}$$

where γ is the ratio of specific heats at constant pressure and constant volume

$$\gamma = \frac{c_p}{c_v} \tag{9}$$

For air at standard conditions, $\gamma = 1.4$.

For completeness, the expressions to determine the primitive variables from F are given below.

$$u = \frac{-\beta - \sqrt{\beta^2 - 4\alpha\delta}}{2\alpha} \tag{10}$$

$$v = \frac{F_3}{F_1} \tag{11}$$

$$\rho = \frac{F_1}{u} \tag{12}$$

$$p = F_2 - \rho u^2 \tag{13}$$

$$e = \frac{p}{\rho\left(\gamma - 1\right)} \tag{14}$$

Where

$$\alpha = -\left(\frac{1}{\gamma - 1} + \frac{1}{2}\right) F_1 \tag{15}$$

$$\beta = \left(\frac{1}{\gamma - 1} + 1\right) F_2 \tag{16}$$

$$\delta = \frac{F_3^2}{2F_1} - F_4 \tag{17}$$

4 Numerical Techniques

4.1 Flow Discretization

The flow field is discretized far in advance of the shuttle to ensure that at the far left side of the grid (i=0), there are free stream flow conditions.

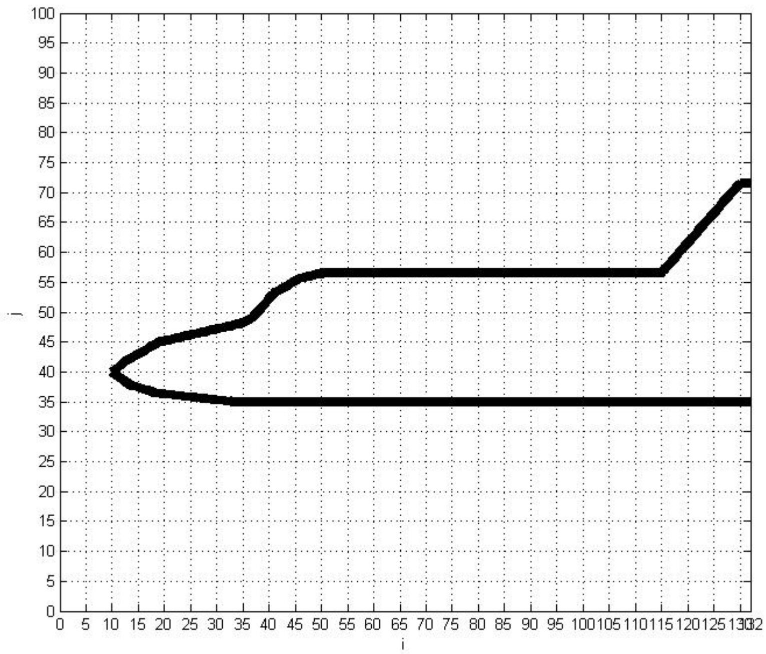

Initial conditions are set for i=0 and the finite difference method described below propagate the flow to the right. So although this is a two dimensional problem, it is very similar to a one dimensional problem with a time evolution. In the figure above, the initial conditions consist of flow corresponding to a high angle of attack. Although the shuttle is aligned with the grid, the flow variables are such that the flow is approaching at a 15 degree angle. The initial conditions are derived from the actual flight reentry profile and are

u=2160 meters/sec v=580 meters/sec

ρ=0.016 kilograms/cubic meter e=167227 joules/kilogram

This approximately corresponds to a flight speed of Mach 7.3 and an altitude of approximately 100,000 feet and is one of the most intense periods of reentry. The primary reason for choosing this flight regime is because it was near this point in reentry that the space shuttle *Colombia* was lost.

4.2 MacCormack's Technique

The dominant finite difference scheme used for shock capturing problems is known as MacCormack's Technique [1]. Developed by Robert MacCormack at NASA Ames Research Center in 1969, MacCormack's Technique was used for the studies of Space Shuttle entry dynamics in the 1970s and 80s.

MacCormack's Technique takes the form of a Predictor-Corrector method. The goal is to propagate downstream according to Equation 7. Using an upwind method for F, the propagation is given by

$$F_{i+1,j} = F_{i,j} + \left(\frac{\partial F}{\partial x}\right)_{ave} \Delta x \tag{18}$$

Since the true value of $\left(\frac{\partial F}{\partial x}\right)$ is not known, a two step process is used to calculate the average value for state propagation.

$$\left(\frac{\partial F}{\partial x}\right)_{ave} = \frac{1}{2}\left[\left(\frac{\partial F}{\partial x}\right)_{i,j} + \left(\frac{\partial \bar{F}}{\partial x}\right)_{i+1,j}\right] \tag{19}$$

4.2.1 Predictor Step

First we calculate the predicted value of $F_{i+1,j}$, denoted $\bar{F}_{i+1,j}$, using $\left(\frac{\partial F}{\partial x}\right)_{i,j}$.

$$\bar{F}_{i+1,j} = F_{i,j} + \left(\frac{\partial F}{\partial x}\right)_{i,j} \Delta x \tag{20}$$

Recall from Equation 7 that

$$\left(\frac{\partial F}{\partial x}\right)_{i,j} = -\left(\frac{\partial H}{\partial x}\right)_{i,j} = -\frac{G_{i,j+1} - G_{i,j}}{\Delta y} \tag{21}$$

Once $\bar{F}_{i+1,j}$ is calculated, it is possible to solve the system of equations for the primitive variables and then construct $\bar{G}_{i+1,j}$.

4.2.2 Corrector Step

We can now find an estimate for $\left(\frac{\partial F}{\partial x}\right)$ at step $i+1$ which can be used to propagate F (and G) according to Equation 18.

$$\left(\frac{\partial \bar{F}}{\partial x}\right)_{i+1,j} = -\frac{\bar{G}_{i+1,j} - \bar{G}_{i,j-1}}{\Delta y} \tag{22}$$

4.3 Boundary Conditions

The boundaries to be concerned with are the top and bottom of the grid as well as the interface with the space shuttle structure. The top and bottom of the grid are considered to be far enough away from the shuttle that they are in the free stream. That is, they are unaffected by the shuttle, thus they can simply be set to the initial conditions. These are Dirichlet boundary conditions.

The fluid flow along a surface must be parallel to that surface. Thus, when the flow intersects the shuttle, the flow velocity must be rotated until it is parallel to the surface. The way the boundary condition is implemented in simulation is by manually specifying the top and bottom edges of the shuttle as well as the desired slope at each point. The rotation is done using a Prandtl-Meyer expansion or compression. Essentially this is a series of shock waves that form to turn the flow through the proper angle. There are tables that specify how the flow parameters change for various turn angles.

4.4 Shock Capturing Technique

A common approach for computing the flow field in the viscinity of shock waves is to consider the shock wave to be a boundary of the computation area. This is because a shock wave is a discontinuity in the solutions. Another approach is known as the Shock Capturing Technique (SCT). In this technique, the grid is extended far outside the region of interest. Shock waves should appear as a blurred area over a few grid points when plotting any of the primitive variables. This is where the variables (u,v,p,etc) have discontinuities. The shock waves do not have to be explicitly assumed, they will appear naturally where they belong. [3] This is the method that I am interested in using for this project.

4.5 Stability Analysis

Because MacCormack's Technique is an explicit finite differences method, it is not necessarily stable for all grid resolutions. [1] Von Neumann stability analysis indicates that the method is stable as long as

$$\frac{\Delta y}{\Delta x} \geq |tan\,(\theta \pm \mu)\,|_{max}. \tag{23}$$

In practice this means that $\frac{\Delta y}{\Delta x}$ must be less than the tangent of the largest turn angle expected. For the space shuttle profile used in this project, keeping this ratio above 2.5 is sufficient.

4.6 Notes on Runtime

The current implementation of this model simulates a 2D shuttle with approximately 480,000 grid points. Runtimes of approximately 2 minutes were experienced. The algorithms implemented here are similar in nature to those used at NASA in the 1970s to do initial simulation of the shuttle design. Using the digital computers of the era, with grid resolutions of approximately 5,000 grid points, the runtime was measured in dozens of minutes [2].

5 Results

Various simulations were performed for different flight attitudes to validate the model as well as determine the effects of various situations on a safe entry. In all cases the grid resolution was set at 800 points in the x direction and 400 in the y direction, with a CFL number of 2.9.

5.1 Nominal Entry

The case of a nominal entry attitude was used to validate the model. An entry angle of attack of 15 degrees was used, and the resulting temperature distribution is shown below.

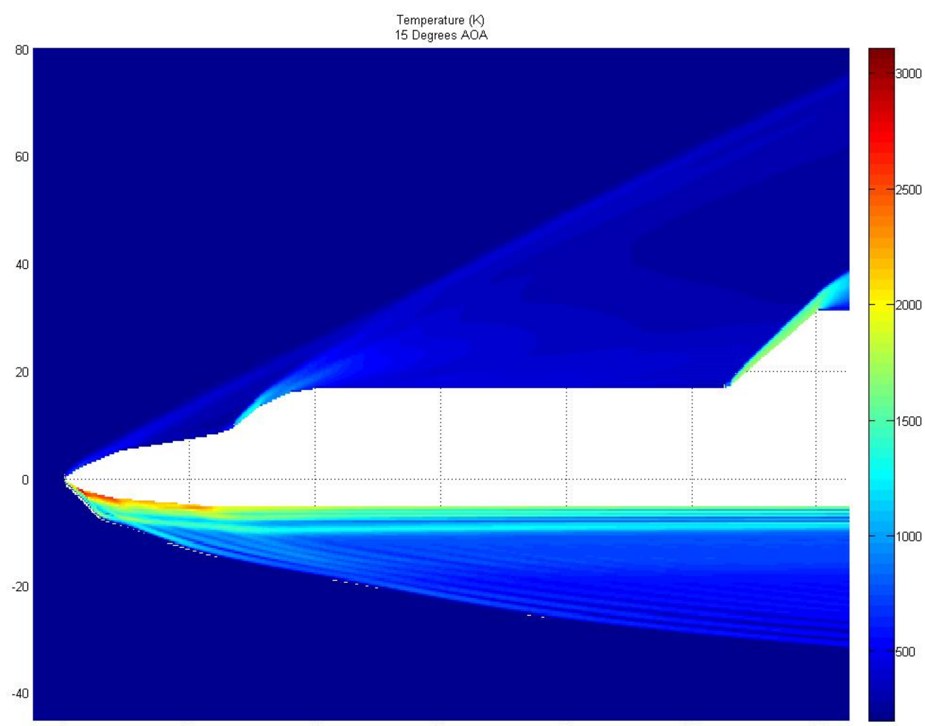

5.1.1 Comparison of Shock Locations with Windtunnel Data

One way to validate the model is to compare the simulated shock locations with experimental data. NASA wind tunnel data for a similarly shaped vehicle is available and is overlayed with the simulated data below. The black squares represent the experimental data at Mach 7.4 and an angle of attack of 15.3 degrees.

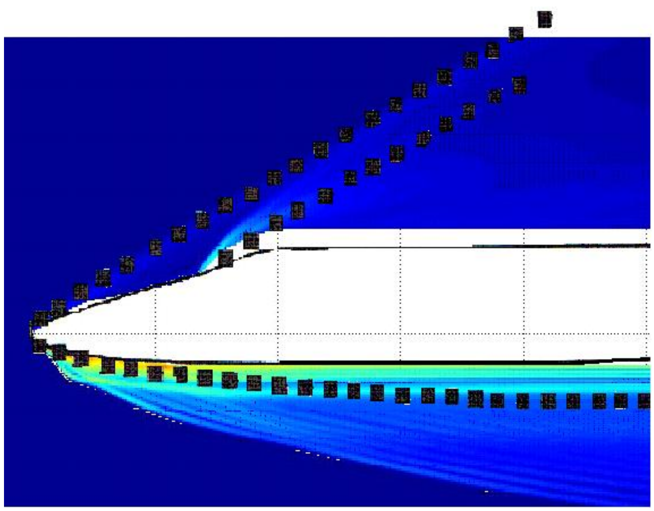

Note that the simulated shock waves match very well with the wind tunnel data. In particular, the top bow wave matches almost perfectly. The dominant shock wave below the vehicle matches very well with experimental data. I believe that the secondary shock wave below the vehicle is much weaker than the higher one and thus would not show up in a wind tunnel experiment. Also note that the geometry of the canopy used in the wind tunnel experiment does not match the true geometry of the shuttle, nor does it match my simulated geometry. The experimental shock forms in much the same manner as the simulated one, but in a slightly different place because of vehicle geometry.

5.1.2 Comparison of Simulated Temperature Distribution with Space Shuttle Thermal Protection System

Note that the temperature distribution is as expected. The underside of the shuttle experiences much more intense heating than the topside. The greatest amount of heating is present just under the nose of the vehicle. Also, the only areas on the top of the shuttle that experience substantial heating are the canopy and the leading edge of the tail. Inspection of the actual space shuttle, shown below, shows that the areas indicated in the simulation match closely with the black areas on the shuttle. The black thermal protection system corresponds to areas of greater heating. Additionally, it is known that the TPS on the underside of the nose is substantially thicker than further back on the vehicle.

The close agreement between the simulated shock locations and the experimental data, as well as the qualitative agreement of the location of orbiter heating serve to validate that the model is performing well.

5.2 Steep Entry Attitude

To test the effectiveness of a blunt body entry, a simulation is run using an angle of attack of only 1 degree.

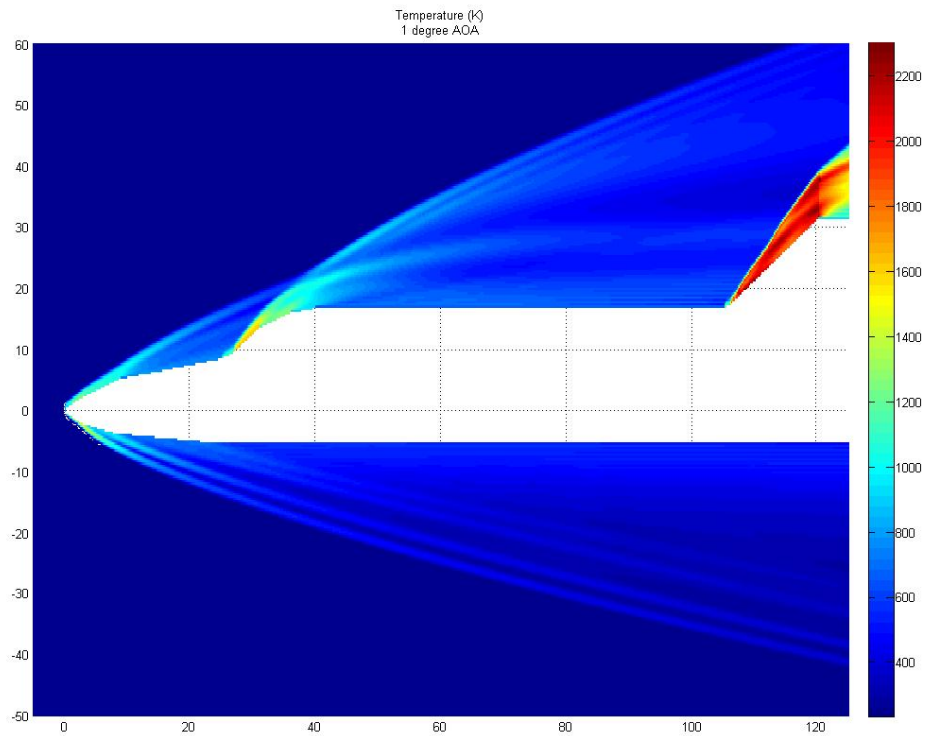

Note that the vehicle is not protected by the blunt body entry effects. The shock waves do not form to dissipate the heat along larger sections of the surface. Instead, heat accumulates at a few points to a very intense degree. In particular, the top of the vehicle takes the brunt of the heating. Because the shuttle lands as an aircraft, the top of the vehicle is where the precious human cargo and payload are located. Additionally, the tail section could not feasibly be reinforced enough to handle that amount of entry heating.

5.3 Protruding Gap Filler

Like any tile system, there exist gaps between the TPS tiles. These gaps are filled with a product known as 'gap filler.' Gap filler is essentially a small carbon sheet that fits between the tiles. On some recent flights the astronauts have observed that the gap filler has become dislodged in a few places during launch. In some instances, the astronauts have actually removed the gap filler to avoid problems during reentry. A photo of protruding gap filler is shown below.

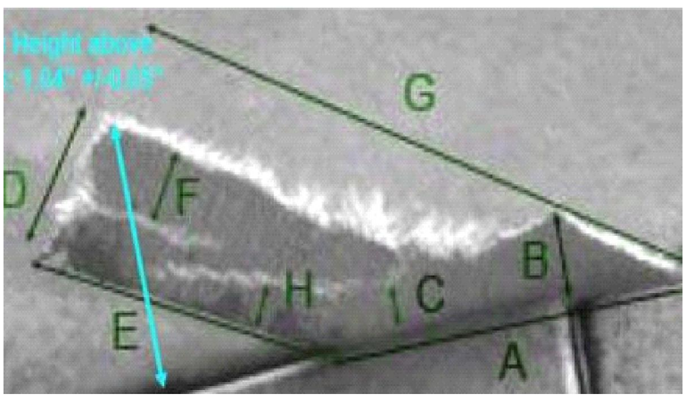

To determine the possible damage a protruding piece of gap filler could cause, a simulation was performed in which a 2 inch thick object protruded 4 inches from the underside of the shuttle. The gap filler is located on a portion of the vehicle that is designed to experience moderate heat.

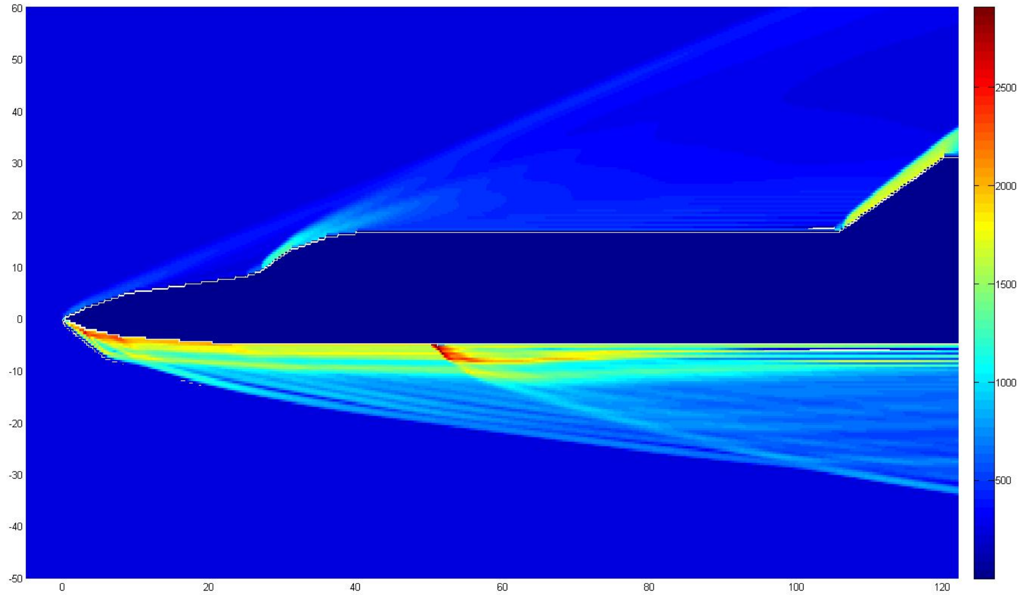

Clearly, a small protrusion on the underside of the space shuttle can cause severe problems. The shock formation is distrupted and a new shock wave intersects the underside of the vehicle. This shock wave causes the vehicle to experience heating comperable to that experienced at the nose. However, the vehicle is not as well protected this far back along the structure. If the protrusion were large enough, and if the tiles around it were damaged at all, this sort of situation could cause severe damage to the orbiter.

6 Conclusions and Suggestions for Future Work

The results presented seem to accurately model the shock wave formation and aerodynamic heating on the space shuttle orbiter during reentry into the Earth's atmosphere. A two dimensional model is presented and validated. Using this model, some insight into the effect of flaws in the thermal protection system as well as the value of a blunt body entry vehicle is achieved.

Improvements to this model should include building a 3D model of the shuttle. The three dimensional algorithm does not appear to be substantially more complicated than the two dimensional one. Instead of beginning with an initial data line, an initial data plane must be specified. There is still no forcing term, so the differential equation is given by Equation 6 with $J = 0$. Additionally, the initial conditions should be further refined. There is limited data available on atmospheric conditions at 100,000 feet, so some educated guesses were made as to the density and energy of the air. Inaccuracies in these estimates may lead to incorrect temperature values in the simulation.

A full 3D model would be useful for testing certain entry dynamics. To slow down during reentry, the space shuttle makes a series of S-turns. In these turns, the shuttle is flying in a high bank angle and the flow is very different from straight forward flight, which was simulated here. It was during one of these turns that they lost contact with *Colombia*, so I think it would be interesting to see how these turns effect the aerodynamics. Additionally, with a 3D model it would be interesting to examine the temperature distribution along the wings, the area that was critically damaged on *Colombia*.

References

[1] John D. Anderson. *Modern Compressible Flow*. McGraw Hill, third edition, 2004.

[2] Paul Kutler and Harvard Lomax. Computation of space shuttle flow fields using noncentered finite-difference schemes. AIAA(73), 1973.

[3] Harvard Lomax and Paul Kutler. Numerical solution for the complete shock wave structure behind supersonic-edge delta wings. 1971.